APPLICATION OF EXPERIMENTAL RESULTS TO NUMERICAL MODELS OF FATIGUE CRACKS PROPAGATING IN THE ROLLING CONTACT ZONE

Paweł Pyrzanowski

Institute of Aeronautics and Applied Mechanics, Warsaw University of Technology
e-mail: pyrzan@meil.pw.edu.pl

The paper presents numerical models of the "squat" type crack serving as an example of the RCF (Rolling Contact Fatigue) crack that appears in railheads. In developing these models, one took into account the results of experimental investigations. Several types of experiments were done: *in situ* measurements of the crack growing rate and the real shape of the contact zone between the worn rail and wheel, measurements of shapes of the real crack in macro- and micro-scales and crack thickness distribution, interactions between crack faces. The results obtained by means of the developed numerical models facilitate understanding of fracture processes and contribute to more precise predictions of the lifetime.

Key words: experimental mechanics, fracture mechanics, rolling contact fatigue, numerical calculations

1. Introduction

The paper is devoted to the problem of fatigue crack propagation in railheads. This type of cracks is often called the Rail Contact Fatigue (RCF) one. The present paper deals with cracks called "squat" or "black spots" that were observed in rails in Poland and in other countries all over the world at the end of the twentieth century. Cracks of this type appeared in tracks in which the rails were made of steel of improved strength properties (resistant to abrasive wear) and had been used about ten years earlier (Kondo *et al.*, 1996; Sawley and Reiff, 2000). The cracks may cause catastrophic accidents of trains, sometimes very dangerous as they can be found in high-speed lines. Figure 1 shows

a top view of a typical large-size singular "squat" type crack, initiated on the rolling strip. The length of this crack on a raceway is about 70 mm.
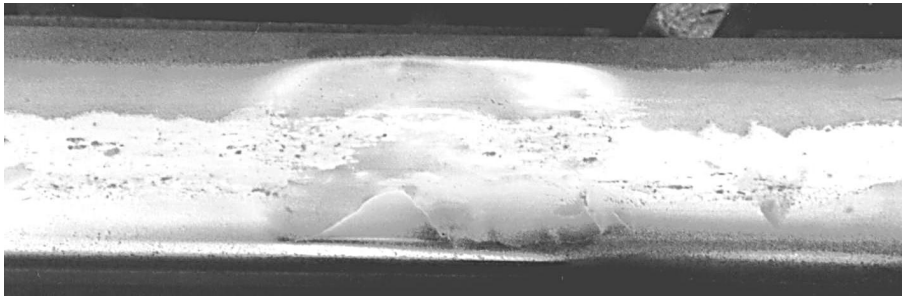

Fig. 1. Top view of a typical large size singular "squat" type crack

These cracks can serve as a good example of a problem to be solved in the field of contact mechanics. The main task is to explain the fatigue crack initiation and propagation under conditions of rolling contact. In many works, propagation of such cracks was described using both two-dimensional models (Bogdański, 2002; Dubourg and Villechaise, 1992; Olzak and Stupnicki, 1999b) and three-dimensional ones (Bogdański *et al.*, 1998; Bogdański and Brown, 2003; Neves *et al.*, 1997). However, some problems still need attention and detailed examination, particularly in view of the fact that the results of recent experimental investigations have not been taken into account in these models.

2. Parameters used in numerical models

Each numerical model should include some parameters the values of which can be assumed, calculated analytically or determined experimentally. Some of the parameters used in the analysis of crack propagation in the contact zone are briefly described below:

- Material properties. Some material constants of the rail steel, like Young's modulus or Poisson's ratio, can be accepted in the same way as for other grades of steel, another parameters must be measured. First of all, these are parameters of stress-strain curves used in elasto-plastic calculations and fracture mechanics parameters like the rate of the crack growth.

- Distribution of the wheel-rail contact stresses. For a new (not exploited yet) rail and wheel, which have nominal shapes of rolling surfaces, geo-

metry of these surfaces is known, and distribution of contact stresses can be calculated form Hertz's equations. For worn rails and wheels, however, the contact problem must be solved numerically or measured experimentally.

- Crack shape. The shape of crack faces both in micro- and macro-scales and the crack thickness distribution must be determined experimentally.

- Crack faces interaction. The interactions between crack faces comprise friction, micro-slip of the crack faces as well as stress concentration near the crack face asperities. They must be measured and they can be represented by a friction coefficient in numerical models.

- Liquid penetration into the crack. The presence of a liquid in the crack brings about significantly different results in comparison with those obtained without the liquid. The presence of the liquid should be verified experimentally.

3.   Experimental determination of parameters

Since some of the parameters necessary for numerical models cannot be assumed in onother way, they should be determined experimentally.

3.1.   Material properties

In rails made of a steel of improved strength properties used in Polish railroads 900A (St90AP) steel has been used. The steel has a chemical constitution given in Table 1 (Żak *et al.*, 2003).

Table 1. Chemical constitution of 900A steel

Element	C	Mn	Si	P	S	Al
Mass fraction [%]	0.7-0.76	1.0-1.25	0.2-0.4	< 0.03	< 0.025	< 0.004

Table 2 contains material properties that were measured by the Author in accordance with the PN-EN Standard for specimens cut off from a railhead.

The results obtained by the Author are similar to those obtained by other researchers, see e.g. Bochenek (1999).

Table 2. Material properties of 900A steel

Parameter	Symbol	Unit	Value	Uncertainty
Young's modulus	E	MPa	192 000	4000
Limit of proportionality	$R_{0.01}$	MPa	500	20
Limit of elasticity	$R_{0.05}$	MPa	600	20
Proof stress	$R_{0.2}$	MPa	730	25
Tensile strength	R_m	MPa	1190	40
Reduction of area at rupture	Z	–	0.42	0.03
Ultimation at rupture	A	–	0.14	0.02

In the course of rolling of a wheel over a rail with a crack, one can observe a very complicated distribution of the stress intensity factors along the crack front. Generally, the crack grows under nonproportional mixed modes I, II, III of load cycles. It is impossible to design an experiment in which the crack front would be loaded in such a way. Most of experiments with mixed mode loadings are performed as proportional I+II, I+III or (very rarely) II+III load cycles. The next problem refers to the material the rails are made of. At present, some experimental results for nonproportional mixed mode I+II cycles for British rail steel BS11 are available (Bold *et al.*, 1991; Brown *et al.*, 1996; Wong *et al.*, 1996). However, some experiments made by the Author proved that the rate of crack growth of Polish rail steel 900A could be 2 to 3 times lower than the same parameter of BS11 steel.

3.2. Distribution of the wheel-rail contact stress

The wear process of wheels and rails changes their geometry and shape of the contact zone. The crack growth changes also the rail geometry. Figure 2 presents the difference between the shape of a rail above the crack and the nominal shape of a UIC60 rail. The lines bear numbers indicating the vertical difference in millimetres.

It can be seen that, for the examined rail, the maximal value of the difference between the nominal and measured shapes of the rail reach about 2.2 mm for regions away from the crack, and 2.6 mm above the crack. This depression of the rail surface is caused by wear observed between the rail and the wheel. In the zone above the crack, wear of crack faces and water penetration into the increasing crack cannot be neglected either. These processes, which lead to a nonzero crack thickness, were presented by Pyrzanowski (2006).
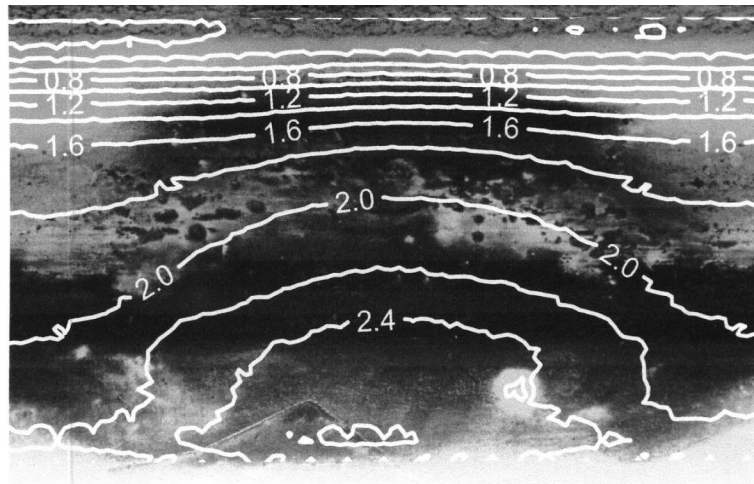
Fig. 2. Difference between the rail shape under a crack and the nominal shape of a UIC60-type rail

Due to changes in the rail height, the shape of the rolling strip is also modified. It is shown in Fig. 3, where measured shapes of rolling strips are indicated as dark areas against the background of a fair rail.
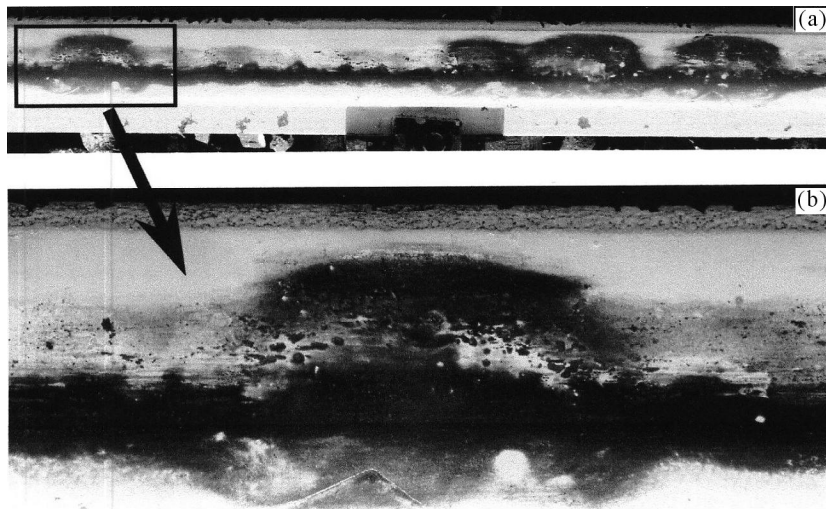

Fig. 3. Measured shape of rolling strips: (a) part of a rail about 800 mm long with four cracks, (b) magnified part of the rail with one crack indicated in Fig. 3a

One rolling strip is divided into two or three parts above the crack (see Fig. 3). The first one is close to the gauge corner, approximately in the same

place as without the crack, and the second one – is near the field corner of
the rail. Consequently, one area of contact pressure is divided into two or
three elements. Figure 4 shows shape of the rolling strip assumed in numerical
calculations and the contact stress distribution calculated for a worn rail and
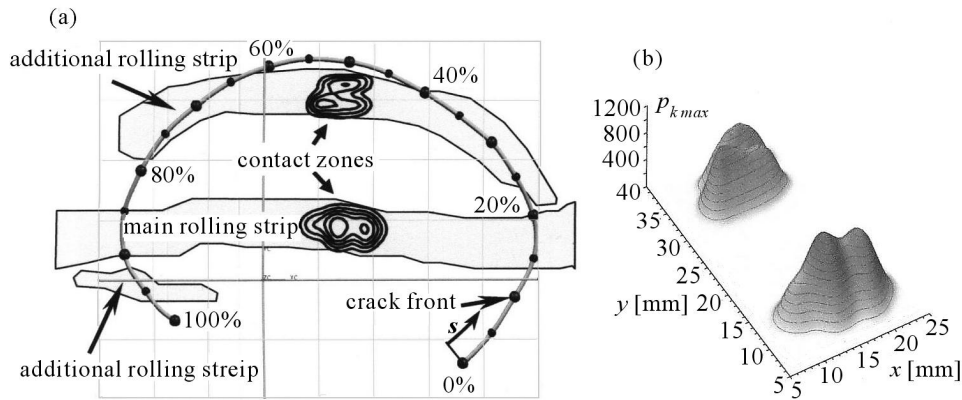wheel for one position of the wheel.

Fig. 4. Distribution of contact stresses: (a) contour map against the background of
rolling strips and crack front, (b) perspective view

The presented distribution of contact stresses cannot be calculated assu-
ming Hertz's theory.

3.3. Shape of the crack

The investigations of the crack shape should address the three following
issues: shape of the crack in macro-scale, shape of the crack faces in micro-scale
(often called roughness) and crack thickness.

3.3.1. Shape of the crack in macro-scale

A very important geometrical problem related to a crack appearing in the
contact zone is its shape. In most of analyses, one assumes a very simple shape
of the crack. For 3D models, it is usually a semi-elliptical shallow-angle part
of a plane, open towards the upper side of the rail in the rail-wheel contact
zone. These models were used by Kaneta and Murakami (1991), Bogdański *et
al.* (1998), Bogdański and Brown (2002). However, experimental investigations
of rolling contact fatigue cracks have proved that their shapes are much more
complicated. The investigations made by the Author (Pyrzanowski and Mruk,
2000) allow one to propose a standard shape of the "squat" type crack as

shown (for a large-size crack) in Fig. 5. The contour lines illustrate the vertical distance from the highest point of the crack face and are drown every 0.25 mm. Grey areas showing real rolling strips depict the wear process. The black bold line, close to the gauge corner of the crack (in the bottom part of the crack in Fig. 5), indicates the crack mouth.
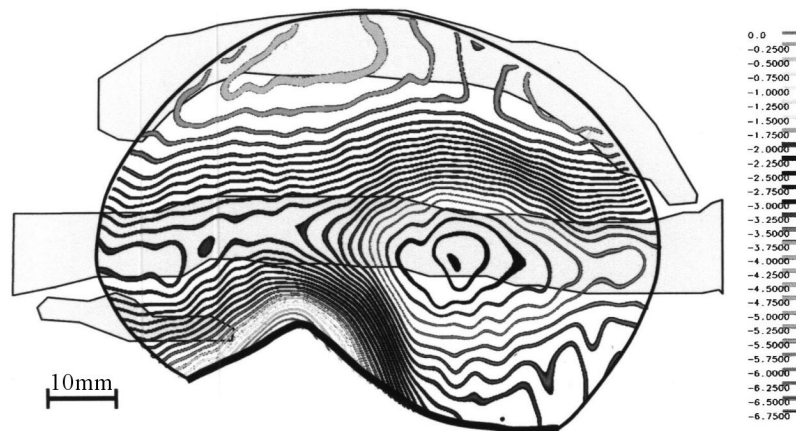

Fig. 5. Standard shape of a "squat" type crack

The measured crack shape was used in numerical models (Pyrzanowski, 2005a,b,c).

Similar profiles of the crack, used in 2D models, are usually very simple and do not correspond to real shapes. These profiles are modelled as straight lines propagating at a shallow angle near the surface (Bower, 1988). A bent crack consists of a few line segments (Dubourg and Villechaise, 1992), a kinked crack with single or double branches (Bogdański, 2002) or a straight line parallel to the rolling surface (Komvopoulos and Cho, 1997). 2D models of rails with cracks can be useful in verification of assumptions or calculations of cases which cannot be solved using 3D models, e.g. with the fluid flow of liquids existing in the cracks. However, the investigations done by Pyrzanowski (2004) show that for 2D models the results very strongly depend on the crack shape, and the real shape cannot be neglected.

3.3.2. Shape of the crack faces in micro-scale

The shape of the crack faces in micro-scale depends on fracture parameters during crack growth and processes that take place in the crack. As shown by Kobayashi *et al.* (1997), it is possible to deduct the load spectrum parameters from fatigue failure surfaces using 3D high-resolution elevation maps.

For cracks appearing in the contact zone, such investigations have not been done yet. Pyrzanowski and Mruk (2000) analysed surfaces of the "squat" type crack using a S3P Penthometer for measuring the distribution of roughness along the base lines 4 mm long situated in various locations on the crack face. Figure 6 presents an exemplary course of crack roughness and histograms of periods of roughness for the some base.
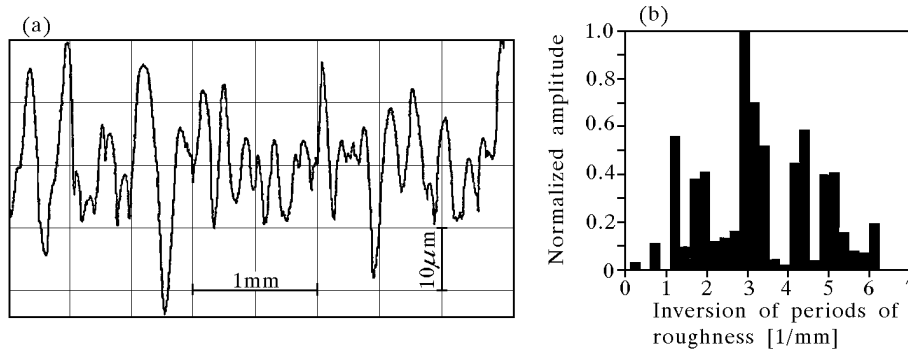

Fig. 6. Crack face roughness: (a) distribution along the base, (b) histogram of roughness

The crack face roughness determined experimentally could be used in numerical calculations (Olzak and Stupnicki, 1999a). In practice, however, it is very complicated.

Olzak and Stupnicki (2001) presented a discussion of two models of crack face interactions, namely, with crack faces covered with layers of a worn out material, the properties of which were determined basing on results of experiments, and with crack faces covered with micro-asperities, which forced crack dilatation accompanying tangential displacements.

All the above-mentioned models used in numerical simulations allow us to draw a conclusion that a more realistic representation of interactions between the crack faces is strongly needed.

3.3.3. Thickness of the crack

The process of thickness formation and growth in a "squat" type crack is stimulated by combined effects of very high contact stresses between a wheel and a rail head, wear process and water penetration into the increasing crack. These processes were accurately described by Pyrzanowski (2006). A simple method was used for measuring the crack thickness, and the results are shown

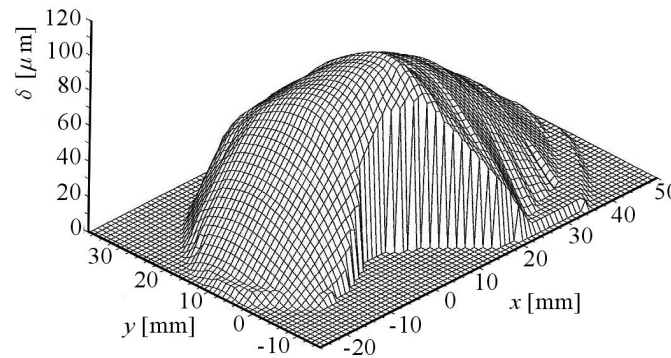in Fig. 7. The calculated volume of the crack was equal to $115 \pm 30 \, \text{mm}^3$ for a crack $77 \, \text{mm}$ long.

Fig. 7. Distribution of crack thickness δ

The knowledge of the crack thickness distribution is very important, especially for cracks appearing within the contact zone, when the crack grows under multimodal conditions with compression stresses normal to the crack faces, or in situations when other effects, e.g. fluid filling, may exist. Numerical calculations (Pyrzanowski, 2004) show that values of stress intensity factors for models with a non zero crack thickness may be a few times higher than those obtained for models with the crack thickness neglected.

3.4. Crack faces interaction

Since the problem of crack face roughness is very complicated in view of both measurement and application, it seems that a better way may be the measuring of interactions between crack faces. Special samples (small cubes) were produced of slices cut out from railheads in which "squat" type cracks were detected. A cube was selected because the investigated crack should be relatively plain and perpendicular to the front surface of the sample. Then, the selected cube was welded by using of a laser beam to the rest of the sample, which then was mounted to the clamping grips. The sample was subjected to normal P_n and tangential P_t forces (see Fig. 8a). The components of the displacement vectors of the sample surface points were registered using the GHI approach with a holographic plate mounted near the sample support point. This method is very convenient, since only one hologram is necessary to obtain the data needed for determination of all three components of the displacement vector, ensuring additionally that the displacements of the sample due to movements of the loading frame are eliminated. Both the registration procedure

of interferograms and the way of their reconstruction were presented in detail by Tu *et al.* (1997) and Szpakowska *et al.* (1998).
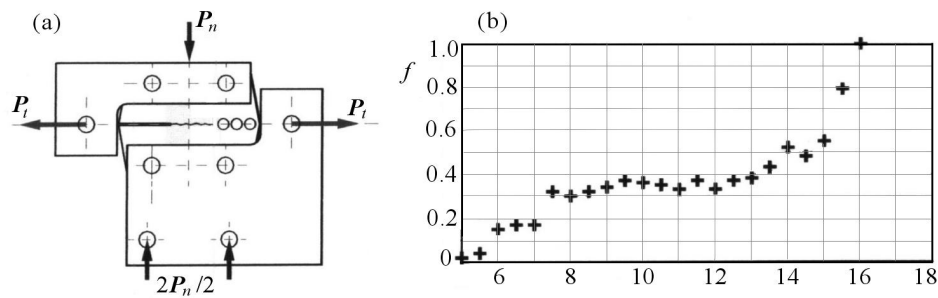

Fig. 8. Crack faces interactions: (a) sample with loading scheme, (b) diagram of the interaction factor f versus crack length

The distribution of the interaction factor f versus the crack length was calculated by means of the loading scheme and analysis procedure described by Pyrzanowski and Stupnicki (2001a,b). The presence of micro-slip between the crack faces causes that the total magnitude of tangential stress tensor ΣS_{xy} is limited for the current total normal stress component ΣS_{yy}, hence the value of the interaction coefficient at a given point of the crack face can be determined as

$$f = \frac{\Sigma S_{xy}}{\Sigma S_{yy}} \tag{3.1}$$

The course of the factor f for the investigated squat-type of crack along its length is presented in Fig. 8b. Its value is relatively small along the greater part of the crack length, and reaching a high value at the crack tip.

The interaction coefficient f can be used as Coulomb's friction coefficient, and its value for the internal part of the "squat" crack can be assumed as 0.35.

3.5. Liquid penetration into the crack

A very important problem arising in railhead cracks consists in penetration of cracks by water (Bogdański *et al.*, 1996; Bower, 1988; Kaneta and Murakami, 1991). The stress intensity factors for cracks filled with water could be much greater than for empty cracks (Pyrzanowski, 2005c). The fact that water does appear in "squat" cracks was proved experimentally. Figure 9 shows traces of the liquid flowing out of the crack (Fig. 9a) and small grains on the crack face (Fig. 9b). These grains are detached from the surface and can be removed by water outflow from the crack. The chemical constitution with a large content

of oxygen shows that the grains consist of iron oxide, which is the product of iron corrosion in the presence of water.
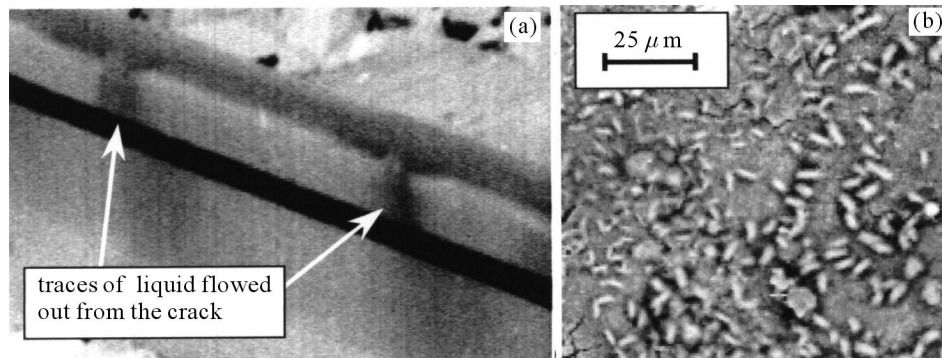

Fig. 9. Evidences of water presence in the crack: (a) traces of the liquid flowed out from the crack, (b) small grains of iron oxide

4. Experimental verification of calculations

The next, very important, role of experiments consists in the verification of models and calculations. These investigations should be done *in situ*, on real objects, loaded in a real manner. For the analysed case, it must be a real "squat" type of crack in a railhead, loaded by an engine. Such investigations can provide, first of all, information about the crack growth rate.

Observation of the crack shape in macro-scale (Fig. 10a) shows visible lines along which the crack front is arrested during summer season. Ultrasound measurements of the crack front position show that the crack grows in the co-planar direction only in the winter season. The knowledge of the load history, i.e. the number of train axles going over the crack (about 27 000 engine axes and 423 000 carriage axles) and the distance between the arrested crack front lines (7 mm) allows us to calculate the average rate of the crack growth. The value of this parameter is 250 to 400 nm/cycle in the direction coincident with the rolling direction of trains.

If the surface of the crack is badly damaged, it becomes difficult to read the crack growth rate. However, for some parts of the crack, it is still possible (see Fig. 10b). The growth rate for the same direction is 250 to 350 nm/cycle.
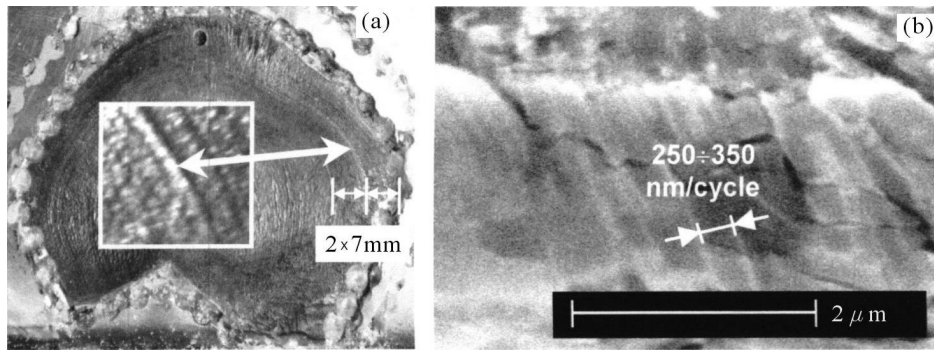
Fig. 10. Experimental verification of the crack growth rate

5. Application of measured parameters to numerical calculations

The measured parameters can be used in numerical calculations. In the most complex model, the real 3D geometry and the existence of water in the crack should be included. Such a model has not been solved yet. In this paper, two models will be briefly discussed: 2D model with 1D liquid flow and 3D one regarding changes of the geometry due to wear.

5.1. 2D model with 1D liquid flow

The advanced model of interaction between a liquid flowing in the crack and crack faces was developed by Olzak and Piechna (2003) and Pyrzanowski and Olzak (2004). Pyrzanowski (2005c) described the same model of the liquid and crack faces interaction in connection with the real geometry of the "squat" crack. In that model, the following assumptions were made:

- A plane specimen was loaded by a rolling cylinder of diameter 900 mm. The maximum contact stresses were 450 MPa which correspond to average stresses between the rail and wheel on a rolling strip.

- Speed of the rolling cylinder was 30 m/s.

- Geometry of the crack corresponded to the measured crack geometry of the rail cross-section under the rolling strip.

- Mechanical thickness of the crack corresponded to the measured one (see Fig. 11).

- Residual hydraulics thickness 30 μm in the vicinity of the crack mouth dropped to 5 μm at the crack front (see Fig. 11).

- The atmospheric pressure was 0.1 MPa at the crack mouth.

- The friction coefficient was equal to zero.

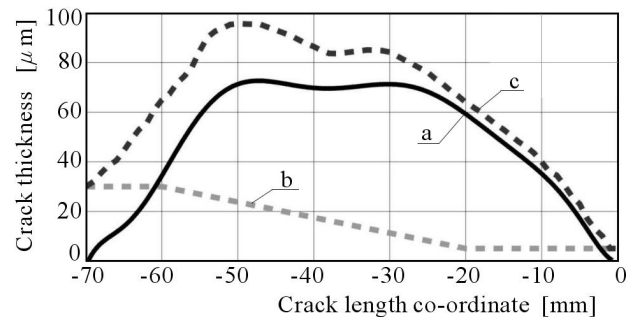- The coefficient of absolute viscosity of the liquid was $0.001\,\mathrm{N\,s/m^2}$.

Fig. 11. Crack thickness: (a) initial mechanical, (b) residual hydraulic, (c) initial total hydraulic

Figure 12 shows some results obtained by means of the presented model. The maximal value of the liquid pressure was 265 MPa (at the crack front, for the cylinder axis 7 mm before crack front – see Fig. 12a) and the maximal value of mechanical thickness of the crack was $111\,\mu$m (12 mm from the crack front for the cylinder axis 30 mm before the crack front – see Fig. 12b).
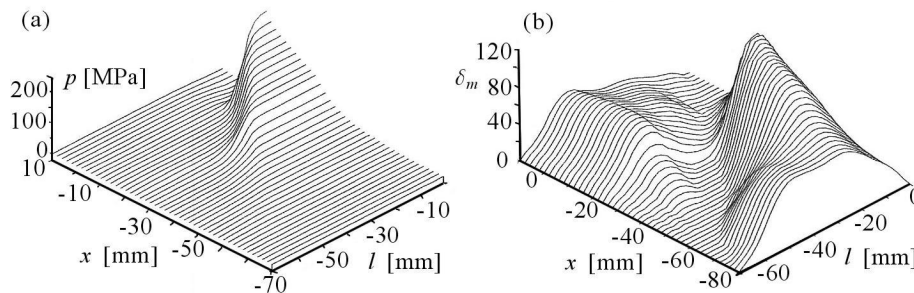

Fig. 12. Distribution of (a) liquid pressure, (b) mechanical thickness versus position along the crack length l and position of the cylinder axis x

Figure 13 depicts the influence of the liquid on the distribution of stress intensity factors during rolling and results for the crack with and without the liquid.

The resulting distributions of stress intensity factors allow one to calculate the crack growth rate. For the crack without the liquid, this value was about
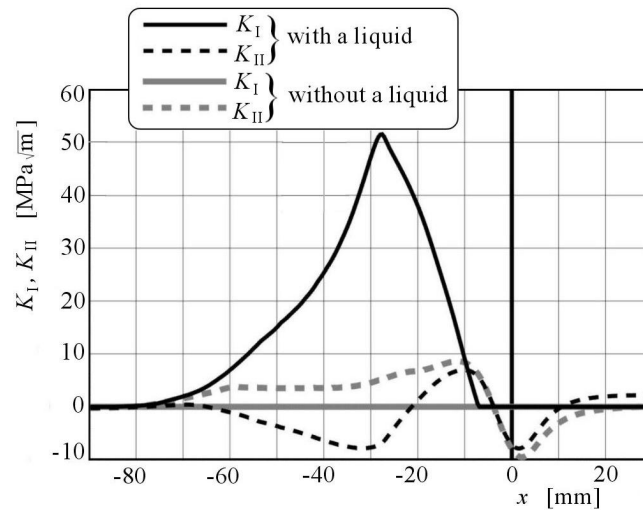
Fig. 13. Distribution of the stress intensity factors K_I and K_{II} during rolling

7 nm/cycle and for the crack with the liquid – about 1200 nm/cycle, assuming that Brown's equations are valid. The value 1200 nm/cycle is 2 to 3 times greater than that observed. The difference between Polish and British steel (described in Section 3.2) or insufficient precision of the assumptions can be the reason for these differences.

5.2. 3D model regarding changes of geometry due to wear process

If the presence of a liquid in the crack is neglected, it becomes possible to solve the problem of the 3D model of a rail with the crack and a wheel. Such a model, in which changes in the geometry caused by wear processes were also introduced, was developed by Pyrzanowski (2000a,c). In this model, real geometry of the rail-wheel contact zone and rolling strips (see Section 3.2 and Fig. 4), shape of the crack in macro-scale (Section 3.3.1 and Fig. 5) and distribution of the crack thickness (Section 3.3.3 and Fig. 7) were taken into account. The finite element model of the rail is shown in Fig. 14. The whole model comprised 83040 elements and 183830 nodes. The crack length was 77 millimetres. The assumed friction coefficient between the rail and wheel was 0.15, and between the crack faces 0.3. The contact load between the rail and wheel was 100 kN, which corresponded to load caused by the engine. The wheel was rolled over the rail over a distance of 110 mm, from the position $x = -43$ mm to $x = 67$ mm (the crack range extended from $x = -27$ mm to $x = 50$ mm – see the crack coordinate system in Fig. 14b).
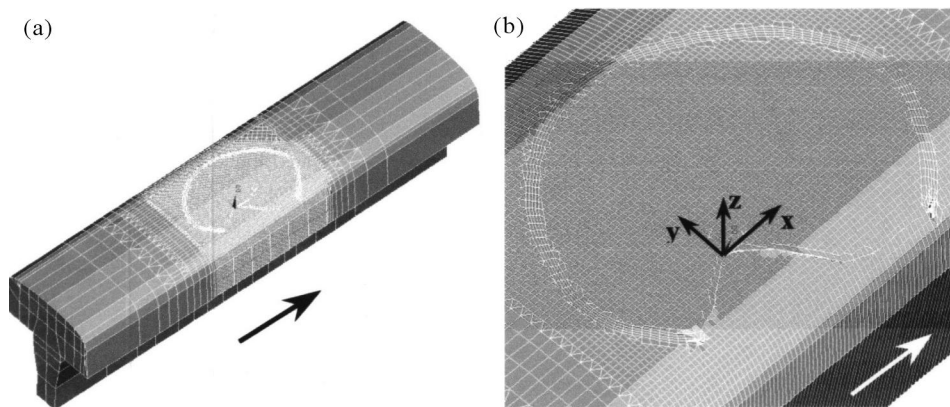
(a) (b)

Fig. 14. A 3D FEM model of a rail with a crack: (a) mesh of the whole rail
(b) magnified mesh over the crack. Arrows indicate the rolling direction of the wheel

As a result, one could calculate the distributions of stress intensity factors versus the position on the crack front s and position of the rail axis in relation to x. Then, the distribution of the crack growth rate along the crack front was calculated (Fig. 15). The presented diagram shows that the co-planar direction of growth is possible only for parts of the crack front in the vicinity of the crack mouth, see grey lines in Fig. 15. For the remaining part of the crack, the calculations show a dominant tendency of branch growing, whose value attains maximum in the front part of the crack just under the rolling strip (black lines in Fig. 15). This corresponds to crack growth in summer, when the crack front is arrested (see Section 4 and Fig. 10a).
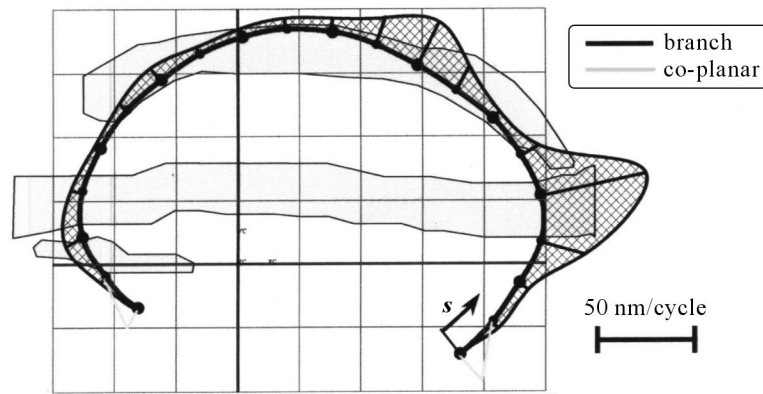

Fig. 15. Distribution of the crack growth rate along the crack front

6. Conclusions

The presented results of experimental investigations and numerical calculations show that at present there exist experimental methods for determination of parameters which are necessary for numerical models of very complicated problems related to cracks existing in the contact zone. Especially, the following parameters should be taken into account:

- Real geometry of bodies in contact, including the effects of wear.
- Geometry of the crack in macro-scale.
- Geometry of crack faces in micro-scale or crack faces interaction.
- Distribution of the crack thickness.
- Influence of other parameters like presence of a liquid, etc.

The computing power of contemporary computers makes it possible to develop very complex 3D models of bodies with cracks.

The results of such calculations can be verified using experimental investigations *in situ*.

References

1. BOCHENEK A., 1999, Badanie przyczyn i sposoby zapobiegania pękaniu szyn UIC obrabianych cieplnie, *Mat. Konf. Eksploatacja szyn UIC60 ulepszanych cieplnie. Problem techniczny, finansowy i społeczny*, Częstochowa, 51-66

2. BOGDAŃSKI S., 2002, The behaviour of kinked RCF cracks in contact, *Proc. 14th European Conference on Fracture*, Cracow, Poland, **I**, 289-296

3. BOGDAŃSKI S., BROWN M.W., 2002, Modelling the three-dimensional behaviour of shallow rolling contact fatigue cracks in rails, *Wear*, **253**, 17-25

4. BOGDAŃSKI S., OLZAK M., STUPNICKI J., 1996, Influence of liquid interaction on propagation of rail contact fatigue cracks, *Proc. of the 2nd Mini Conference on Contact Mechanics and Wear of Rail/Wheel Systems*, Budapest, 134-143

5. BOGDAŃSKI S., OLZAK M., STUPNICKI J., 1998, Numerical modelling of a 3D rail RCF "squat"-type crack under operating load, *Fatigue and Fracture of Engineering Materials and Structures*, **21**, 923-935

6. BOLD P.E., BROWN M.W., ALLEN R.J., 1991, Shear crack growth and rolling contact fatigue, *Wear*, **144**, 307-317

7. BOWER A.F., 1988, The influence of crack face friction and trapped fluid on surface initiated rolling contact fatigue cracks, *ASME J. of Tribology*, **110**, 704-710

8. BROWN M.W., HEMSWORTH S., WONG S.L., ALLEN R.J., 1996, Rolling contact fatigue crack growth in rail steel, *Proc. of the 2nd Mini Conference on Contact Mechanics and Wear of Rail/Wheel Systems*, Budapest, 144-153

9. DUBOURG M.C., VILLECHAISE B., 1992, Stress intensity factors in a bent crack: a model, *European Journ. of Mechanics A/Solids*, **11**, 2, 169-177

10. KANETA M., MURAKAMI Y., 1991, Propagation of semi-elliptical surface cracks in lubricated rolling/sliding elliptical contacts, *ASME J. of Tribology*, **113**, 270-275

11. KOBAYASHI T., SHOCKEY D.A., SCHMIDT C.G., KLOPP R.W., 1997, Assessment of fatigue load spectrum from fracture surface topography, *Int. J. of Fatigue*, **19**, supp. 1, 237-244

12. KOMVOPOULOS K., CHO S.S., 1997, Finite element analysis of subsurface crack propagation in a half-space due to a moving asperity contact, *Wear*, **209**, 57-68

13. KONDO K., YOROIZAKA K., SATO Y., 1996, Cause, increase, diagnosis, countermeasures and elimination of Shinkansen shelling, *Wear*, **191**, 199-203

14. NEVES A., NIKU S.M., BAYNHAM J.M.W., ADEY R.A., 1997, Automatic 3D crack growth using BEASY, *Proc. 19th Boundary Element Method Conf., Computational Mechanics Publications*, Southampton, 819-827

15. OLZAK M., PIECHNA J., 2003, Numeryczna analiza wpływu cieczy na zmęczeniowy rozwój pęknięcia typu "squat" w bieżni szyny kolejowej, *Mat. IX Krajowej Konf. Mechaniki Pękania*, Kielce-Cedzyna, 2003, *Zeszyty Nauk. Politechniki Świętokrzyskiej, Mechanika*, **78**, 381-393

16. OLZAK M., PYRZANOWSKI P., STUPNICKI J., 2001, Rolling contact problem – fatigue crack propagation in a surface layer, *Journal of Theoretical and Applied Mechanics*, **39**, 3, 589-620

17. OLZAK M., STUPNICKI J., 1999a, Fluctuation of the stress intensity factors under a load rolling over a race way with a crack. Part I: crack with uneven faces, *Mat. VII Krajowej Konferencji Mechaniki Pękania*, Kielce-Cedzyna, tom II, 109-116 (in Polish)

18. OLZAK M., STUPNICKI J., 1999b, The influence of crack faces interaction model on the results of numerical study of stress intensity factors for the surface breaking cracks in race way, *Proc. IV Conf. on Computational Methods in Contact Mechanics*, Stuttgart, Germany, 109-118

19. OLZAK M., STUPNICKI J., 2001, Numerical study of the Stress Intensity Factors for cracks in raceways with the experimentally determined interaction between crack faces, *Proc. of Conference on Contact Mechanics*, Sevilla, Spain, 253-262

20. Pyrzanowski P., 2004, Influence of a subsurface fatigue crack on stress distribution due to rolling contact: experimental verification of numerical results, *The Archive of Mechanical Engineering*, **LI**, 3, 335-359

21. Pyrzanowski P., 2005a, 3D models of "sqat" type fatigue cracks growed in the rail heads, *Proc. of III Sympozjum Mechaniki Zniszczenia Materiałów i Konstrukcji*, Augustów, 317-322 (in Polish)

22. Pyrzanowski P., 2005b, Influence of wear of the rolling surface on development of fatigue cracks in the contact zone, *Proc. of X Conference on Fracture Mechanics*, Wisła, *Zeszyty Naukowe Politechniki Opolskiej*, **83**, 305, vol. 2, 185-192 (in Polish)

23. Pyrzanowski P., 2005c, Modelling of the fatigue cracks propagating in the rolling contact zone, *Mechanics*, **208**, Oficyna Wyd. Politechniki Warszawskiej, (in Polish)

24. Pyrzanowski P., 2006, Estimation and consequences of the crack thickness parameter in the assessment of crack growth behaviour of " "squat" type cracks in the rail-wheel contact zone, *Engineering Fracture Mechanics* (in press)

25. Pyrzanowski P., Mruk I., 2000, Investigation of "squat"-type crack development in heads of rails, *Proc. of 17th Danubia-Adria Symposium on Experimental Methods in Solid Mechanics*, Praga, Czech Republic, 281-284

26. Pyrzanowski P., Olzak M., 2004, Wpływ cieczy wypełniającej szczelinę na parametry mechaniki pękania podczas przetaczania obciążenia, *Mat. XX Symp. Zmęczenia i Mechaniki Pękania*, Bydgoszcz-Pieczyska, 339-356

27. Pyrzanowski P., Stupnicki J., 2001a, Evaluation of contact rigidity of fatigue crack faces for numerical models of RCF crack growth, *Proc. of GESA Symposium 2001*, VDI Berichte 1599, Chemnitz, Germany, 353-361

28. Pyrzanowski P., Stupnicki J., 2001b, Interaction between the faces of a squat-type fatigue crack determined by use of the grating holographic interferometry, *Proc. of 14th European Conference on Fracture*, Kraków, **II**, 713-723

29. Sawley K., Reiff R., 2000, Rail Failure Assessment for the Office of the Rail Regulator. An assessment of Railtrack's methods for managing broken and defective rail. Report no. P-00-070, Transportation Technology Center, Inc. A subsidiary of the Association of American Railroads, Pueblo, Colorado, USA

30. Szpakowska M., Pyrzanowski P., Stupnicki J., 1998, Interference of fracture surfaces observed by means of optical methods for the cracks subjected to shear and compression, *Proc. of IUTAM Symposium Advanced Optical Methods and Application in Solid Mechanics*, Poitiers, France, **2**, L. 37, 1-12

31. Tu M., Gielisse P.J., Xu W., 1997, Grating Holographic Interferometry, *Experimental Mechanics*, **37**, 2, 188-196

32. Wong S.L., Bold P.E., Brown M.W., Allen R.J., 1996, A branch criterion for shallow angled rolling contact fatigue cracks in rails, *Wear.* **191**, 45-53

33. Żak S., Sarna J., Merta J., 2003, Ocena jakości szyn produkcji Huty Katowice, *Mat. XXII Konf. Nauk.-Techn. Huty Katowice – Produkcja i eksploatacja szyn kolejowych*, Rogoźnik, 32-48

Wykorzystanie wyników badań eksperymentalnych w modelach numerycznych pęknięć zmęczeniowych rozwijających się w strefie kontaktu tocznego

Streszczenie

W pracy opisano modele numeryczne pęknięć zmęczeniowych typu "squat" rozwijających się w strefie kontaktu tocznego koło-szyna w główkach szyn kolejowych. Przy tworzeniu tych modeli wykorzystano wyniki badań eksperymentalnych. Opisano następujące eksperymenty: badania terenowe prędkości rozwoju pęknięcia oraz kształtu szczeliny w makro- i mikroskali oraz grubości szczeliny, a także pomiar oddziaływania pomiędzy brzegami pęknięcia. Uwzględnienie w obliczeniach wyników badań eksperymentalnych pozwala bardziej wiarygodnie prognozować rozwój pęknięć i czas dopuszczalnej eksploatacji szyn.